Electron-energy-loss study of the oxidation of polycrystalline tin

Gar B. Hoflund and Gregory R. Corallo
Department of Chemical Engineering, University of Florida, Gainesville, Florida 32611
(Received 13 January 1992)

An electron-energy-loss (EELS) study has been carried out on polycrystalline Sn before and after room-temperature exposures of 100, 500, 1500, and 3500 L [1 Langmuir (L)=10^{-6} Torr s] to O_2 at low pressure (10^{-6} Torr) and to O_2 at high pressures (160 Torr for 5 min and air at 1 atm for 5 min). Depth-sensitive information was obtained from these surfaces by varying the primary-electron-beam energy from 100 to 600 eV and using inelastic mean-free-path calculations. The spectra have been interpreted based on features in the EELS spectra obtained from standard reference materials; Sn metal, SnO, and SnO_2. During the 100-L exposure, O_2 adsorbs dissociatively and forms SnO in the near-surface region. Subsurface SnO forms more deeply beneath the surface during the 500-L exposure, and a subsurface transitional oxide structure with a composition between that of SnO and SnO_2 also forms. Higher exposures up to the EELS saturation exposure of 3500 L converts some of this transitional phase into subsurface SnO_2. Angle-resolved EELS shows that the very near-surface region (outermost two or three atomic layers) consists almost entirely of SnO with Sn metal, transitional oxide, and SnO_2 lying beneath the surface after a low-pressure, saturation exposure to O_2. After a high-pressure exposure, the near-surface region is fully oxidized to a mixture of SnO and SnO_2 with no metallic Sn. The SnO_2 concentration is maximum at about 1.4 nm beneath the surface, and both SnO and transitional oxide are present throughout the 3.0-nm oxidized layer in varying quantities. The presence of moisture appears to accelerate the oxidation process in some undetermined manner.

INTRODUCTION

Since tin metal and its oxides are technologically important in many application areas relating to semiconductor devices, solar energy cells, heterogeneous catalysts, and protective coatings, it is important to understand the oxidative behavior of polycrystalline tin. Consequently, the oxidation of tin has been investigated in numerous studies.[1-7] This is a difficult system to study because it is not easy to distinguish between the two stable oxides SnO and SnO_2 and methods are required that yield both composition and chemical state information as a function of depth. Electron spectroscopy for chemical analysis (ESCA or x-ray photoemission spectroscopy) can be used to distinguish between metallic Sn, which has a $3d_{5/2}$ binding energy of 484.6 eV, and Sn oxides (SnO and SnO_2), which have a $3d_{5/2}$ binding energy of 486.4 eV. Earlier studies[8-10] have not found a difference in $3d_{5/2}$ binding energies between SnO and SnO_2, but recently Paparazzo *et al.*[11] claim that they differ by 0.19 eV based on ESCA data obtained using a monochromatized x-ray source. It is possible to distinguish between SnO and SnO_2 using valence-band ESCA or ultraviolet photoemission spectroscopy.[2,8,12,13] Auger electron spectroscopy (AES) has also been used to examine the O/Sn system.[1,2,9,14,15] In most studies, identical Auger peak shifts have been observed for SnO and SnO_2. The extent of the shift for the $M_4N_{4,5}N_{4,5}$ Auger transitions varies between the different studies; Asbury and Hoflund[1] and Lin, Armstrong, and Kuwana[9] observed a shift of 5 eV from metal to oxide, Powell[2] measured a shift of 5.5 eV, and Wagner and Biloen[15] found a shift of 3.9 eV, whereas Sen, Sen, and Bauer[14] claim to have observed a shift of 3 eV for SnO and 7 eV for SnO_2.

Based on these ESCA and AES results, it appears that the power of these techniques for examining the oxidation of Sn is limited. However, electron-energy-loss spectroscopy (EELS) is able to distinguish between SnO and SnO_2,[2,5,12] and its depth sensitivity can be varied by changing the primary-beam energy[12] or the incidence and collection angles.[16] EELS has been used by Woods and Hopkins,[7] Bevolo, Verhoeven, and Noack,[4,5] Stander,[3] and Powell[2] to study the oxidation of Sn, but the interpretations of the results are quite varied. This is probably due to the complexity of EELS data, the difficulty involved in making peak assignments, and the fact that complete data sets have not been taken. Woods and Hopkins[7] performed EELS using a single primary-beam energy of 70 eV. Based on low-energy electron diffraction, AES, and EELS data, they suggest that a single monolayer of SnO forms on Sn(001) after a low-pressure, room-temperature, saturation dose (approximately 2500 L) of O_2. [1 Langmuir (L)=10^{-6} Torr s.] Bevolo, Verhoeven and Noack[5] present limited depth-sensitive EELS data taken using two primary-beam energies, 75 and 400 eV, with varying incidence angle. They suggest that continuous-oxide films free of metallic Sn are grown following O_2 exposures of $100-10^7$ L. They also claim that SnO_2 and SnO are present in any oxide layer and that the near-surface region is SnO_2 rich. Furthermore, these authors observe the simultaneous presence of a metallic-surface plasmon and an oxidic-surface plasmon following an exposure of less than 100 L so they propose that island growth of the oxide occurs at low coverage.

 ©1992 The American Physical Society

Powell[2] examined the oxidation of Sn using numerous techniques including UPS, ESCA, AES, work-function measurements, and EELS using a single primary-beam energy of 400 eV. He suggests that a metallic surface may be present, below which lies SnO according to the EELS data. However, the UPS data indicate that SnO_2 is also present following a low-pressure exposure. In an EELS study using a single primary-beam energy of 435 eV, Stander[3] proposes that a highly nonstoichiometric SnO_2 layer forms during the initial stages of oxidation and that the outermost layer remains metallic. This supports the previous suggestion by Powell.[2]

Although many important questions still need to be resolved, these studies demonstrate that EELS is a powerful technique for examining the oxidation of Sn. The purpose of this present study is to present and describe EELS data in which the primary-beam energy, experimental geometry, and O_2 exposures are varied systematically over a wide range in order to gain a better understanding of the oxidation of Sn. From this EELS data it has been possible to construct a semiquantitative plot of the Sn oxidation state as a function of depth for O_2 exposures of 100, 500, 1500, and 3500 L at 10^{-6} Torr, 160 Torr for 5 min, and a 5-min air exposure.

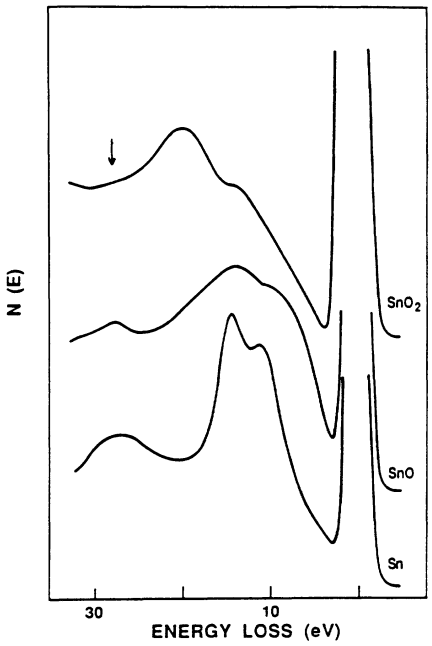

FIG. 1. EELS spectra obtained from standard samples including sputter-cleaned polycrystalline Sn metal, SnO powder, and SnO_2 powder using a 400-eV primary-electron beam. This figure has been reproduced from the study by Powell (Ref. 2).

EXPERIMENT

A polycrystalline Sn foil (7×10×0.25 mm) of 99.9995% purity was used in this study. The sample was ultrasonically solvent cleaned in toluene, trichloroethylene, acetone, and ethanol prior to insertion into the ultrahigh-vacuum chamber. After pumpdown to a base pressure of 1×10^{-10} Torr, the sample was sputtered with 2 keV Ar^+ until the C and O contaminants were removed. An Auger spectrum obtained from the cleaned Sn surface is shown in Fig. 1 of a previous EELS study.[16] Auger spectra were obtained using a 3-keV primary-beam energy and operating the cylindrical mirror analyzer (CMA) (PHI model 25-270 AR) in the nonretarding mode. Lock-in detection was used with a 0.5 V_{pp} sine wave of 10-kHz frequency applied to the outer cylinder of the CMA.

EELS was performed by operating the CMA in the retarding mode with a pass energy of 25 eV ($\Delta E/E_{\text{pass}}=0.016$) and using digital pulse counting.[17] Ten 2000-channel spectra were taken over a 50-eV energy range with a maximum capacity of 8000 counts in a channel. The summation of these spectra was then averaged with a spline quadratic fit to obtain the EELS spectra presented in this paper. A primary-beam current of 100 nA over a spot size approximately 0.5 mm in diameter was used. The full width at half maximum of the elastic peak decreased from 0.82 eV at $E_p=600$ eV to 0.52 eV at $E_p=100$ eV. Angle-resolved EELS (AREELS) spectra were taken by tilting the sample about 45° with respect to the CMA axis and using the 90° movable aperture to select the collection angle. Using the electron gun in the CMA provided an incidence angle of 45°. In the angle-integrated mode, electrons were collected in a 360° cone which makes an angle of 42.3° with respect to the sample normal when the sample surface is normal to the axis of the CMA. Unless stated otherwise, EELS data were taken in the angle-integrated mode. The sample was sputter cleaned after each exposure. Most of the EELS spectra were also collected in another vacuum system described previously[12,18] and found to be reproducible.

RESULTS AND DISCUSSION

Reference EELS spectra taken by Powell[2] from Sn metal, SnO, and SnO_2 using a 400-eV primary-beam energy are shown in Fig. 1. The three spectra clearly are quite different and form a basis for distinguishing between these chemical states of Sn. The two oxide spectra were obtained from high-purity powders with bulk compositions of SnO and SnO_2. Although it is usually quite difficult to prepare standards with known surface compositions, Powell argues that low-energy (<1 keV) ion sputtering does not reduce SnO_2. However, Cox and Hoflund[12] show that the near-surface region of a tin oxide film is damaged during sputtering with consequential changes in the EELS spectra particularly for those obtained using low primary-beam energies. This study and another by Tarlov and Evans[19] show that oxygen is selectively removed from tin oxide surfaces by ion sputtering. The fact that Powell collected the reference spectra shown in Fig. 1 using a 400-eV primary beam minimizes the influence of sputter damage on the oxide spectra because a 400-eV beam probes fairly deeply beneath the surface as discussed below. This statement is supported by the fact that a well-defined, prominent 27-eV peak,

which is characteristic of SnO, does not appear in the spectrum obtained from SnO_2. However, a small 27-eV shoulder denoted by an arrow appears on the large 20-eV SnO_2 feature. This is probably due to SnO lying at the surface, which was produced during sputtering. Also, the small peak at 13 eV may be due to the presence of this SnO. Therefore, it probably is not possible to prepare an SnO_2 standard surface by sputtering SnO_2. However, it may be possible to produce such a surface by sputtering a thin film of Sn onto Cu in the presence of 10 Torr of O_2 at 200 °C and then annealing at some high temperature in a high pressure of O_2. The absence of SnO could be determined using EELS since no 27-eV EELS peak would appear for a tin oxide film containing only SnO_2. SnO would not be as susceptible to reduction to Sn by sputtering as reduction of SnO_2 is to SnO. Therefore, the SnO spectrum most likely is quite representative of one which would be obtained from a true SnO standard, particularly since a 400-eV primary beam, which probed beneath the sputter-damaged region, was used.

Assignment of the peaks in the Sn metal, SnO, and SnO_2 EELS spectra is very difficult, particularly for the oxides, and has been addressed to some extent in each Sn-related EELS study. It is generally accepted that the peaks are due to either interband or intraband excitations or surface or bulk-plasmon losses, but distinguishing between these possibilities is not straightforward and making such assignments usually requires some speculation. At this point, the peaks in the metallic Sn EELS spectrum are well understood and have been carefully discussed in the previous part of this study[16] and other Sn EELS studies.[2–7] The predominant peaks are due to surface- and bulk-plasmon losses at 10 and 14 eV ($\sim\sqrt{2}\times 10$ eV) respectively. This is reasonable since Sn has a metallic nature and the nearly free electrons comprising the conduction bands give rise to the plasmon excitations. Multiple-plasmon loss features have also been resolved[16] including a bulk-bulk loss at 28 eV, a bulk-surface loss at 24 eV, a surface-surface loss at 20 eV, and triple plasmon features at higher-loss energies. These assignments were tested by varying the surface sensitivity of the EELS experiment by changing either the primary-beam energy and/or the incidence and collection angles in an AREELS experiment.[16] The features change appropriately in that the peaks associated with the surface plasmon increase in magnitude with respect to the peaks associated with the bulk plasmon as the primary-beam energy decreases or the incident or collection angles become more grazing, i.e., as the surface sensitivity of the EELS experiment increases. This method of testing assignments is quite important since it is one of the few ways available. A small feature also appears in many of the EELS spectra obtained from metallic Sn at about 5.5 eV. Bayat-Mokhtari, Barhovv, and Gallon[20] have assigned this feature (4.7 eV according to their loss energy assignment technique) as an interband transition, which is consistent with the results of an optical-absorption study of Rasigni *et al.*[21] Comparison of EELS spectra with optical-absorption data allows a distinction to be made between plasmon and electron excitations because photons do not excite plasmon modes. However, this fact has not been utilized much in EELS studies. The 5.5-eV feature may be due to an excitation from a filled Sn 5*s* level to an unoccupied Sn 5*p* level. Both the absolute and the relative sizes of the features due to particle (single electron) and collective (plasmon) excitations are important with regard to understanding the EELS spectra obtained from clean and oxidized Sn. Unfortunately, the intensity variations are complicated and only minimal effort has been spent thus far in examining these variations systematically. For metallic Sn the plasmon-loss features are much larger than the features due to particle excitations. The interband transition peak at 5.5 eV becomes more apparent in the surface-sensitive EELS spectra, in which the intensities of the plasmon features are decreased particularly for rough surfaces. Peaks due to other particle excitations must be present, but these are not apparent because they are overlapped and dominated by the plasmon features. Assignment of the oxidic EELS features are even more complex and have been controversial. Powell[2] and Bevolo, Verhoeven, and Noack[5] have suggested that the predominant loss features in the SnO and SnO_2 EELS spectra are due to plasmon excitations whereas Cox and Hoflund[12] have argued that they may be due to single-particle excitations since the electrons are more localized in the oxides and may not oscillate in a collective manner as in a metal.

In interpreting the EELS data presented below to obtain Sn chemical-state information as a function of depth for various O_2 exposures, it is not necessary to know the loss mechanism responsible for producing each of the peaks in the Sn, SnO, and SnO_2 EELS spectra. However, it is important to know which peaks are present in each standard spectrum and their energies, and it is preferable to have some information about their intensities as a function of primary-beam energy. Considering the previous EELS studies, it seems that this information is available, but there are several complicating factors to consider. Firstly, the energy resolution of the Sn EELS studies has often been low enough so that some spectral features have not been discerned. For example, the spectra shown in Fig. 1 were taken using a single-pass CMA in the nonretarding mode. These spectra exhibit broad features compared to spectra taken using a double-pass CMA in the retarding mode (Refs. 12 and 16 and this study). A wide and rather structureless feature appears in the SnO reference spectrum between about 3 and 23 eV. More and better-defined features are observed in similar spectra presented in the study by Cox and Hoflund.[12] The 27-eV peak due solely to SnO is also much sharper than that shown in Fig. 1. In this present study, the features primarily used to identify the presence of various Sn species are Sn—10 eV, 14 eV, SnO—9 eV, 13.5 eV, 27 eV, and SnO_2—20 eV. In some cases less significant features may also provide useful information.

Secondly, the EELS data in this study are analyzed assuming that bulklike Sn, SnO, and SnO_2 phases are present. Suboxides have been observed after exposing polycrystalline Sn to O_2 at low pressure in a study by Asbury and Hoflund,[1] but no EELS data from these species are available. Their EELS spectra may be similar to SnO,

in which case they would be classified as SnO in this study. Reduction of tin oxide films by 2-keV Ar-ion bombardment has also been demonstrated,[12,19] and the damaged layers produced yield altered EELS spectra. It is possible that defect-laden SnO_2 or SnO phases may form during oxidation. In a study of tin oxide surfaces, Cox and Hoflund[12] have attributed the presence of an 18-eV tin oxide-loss feature to a defect structure with a composition between that of bulk SnO_2 and surface SnO. As discussed below, this phase is found in the oxidation of Sn also.

Thirdly, little is known about intensities of features from the various species present during the oxidation of Sn and the variations of these intensities with primary-beam energy. One helpful fact can be gained from Fig. 3 of the study by Powell,[2] which shows the magnitude of EELS features obtained from the Sn, SnO, and SnO_2 standards normalized to the same 400-eV elastic peak height. The surface and bulk plasmon losses from Sn metal appear to be about five times as intense as the predominant oxidic-loss features. This fact supports the assertion made above that the metallic-plasmon losses probably are so large that they obscure the losses due to single-particle excitations.

EELS spectra obtained from polycrystalline Sn after exposure to O_2 (10^{-6} Torr) for 100, 500, 1500, and 3500 L, 160 Torr of O_2 for 5 min, and 160 Torr of air pressure for 5 min are shown in Figs. 2–7, respectively. Each set of spectra was obtained using primary-electron-beam energies of 100, 200, 400, and 600 eV. As the primary-beam energy increases, the depth probed increases. This important topic is discussed more quantitatively below. No changes in the EELS spectra are observed with low-pressure exposures greater than 3500 L. This EELS saturation exposure compares favorably with the AES saturation value of 5000 L (Ref. 2) and the UPS saturation value of 4000 L.[13] In order to better understand this complex set of EELS spectra, the spectral variations with exposure for each primary-beam energy is shown in Figs. 8–11. The corresponding EELS spectra obtained from

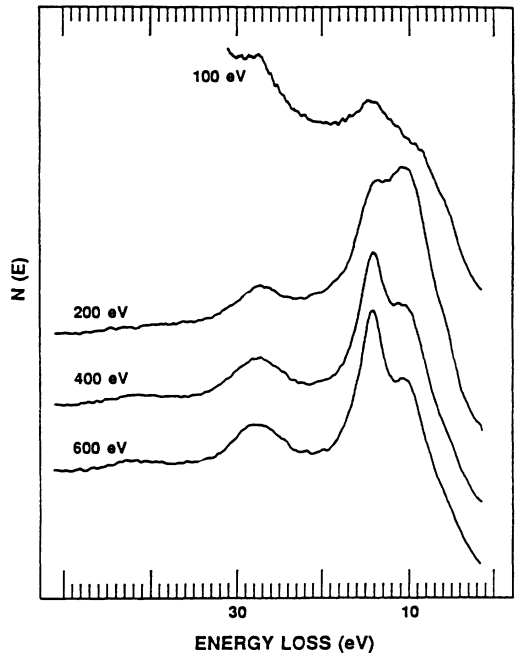

FIG. 3. EELS spectra obtained from polycrystalline Sn after exposure to 500 L of O_2.

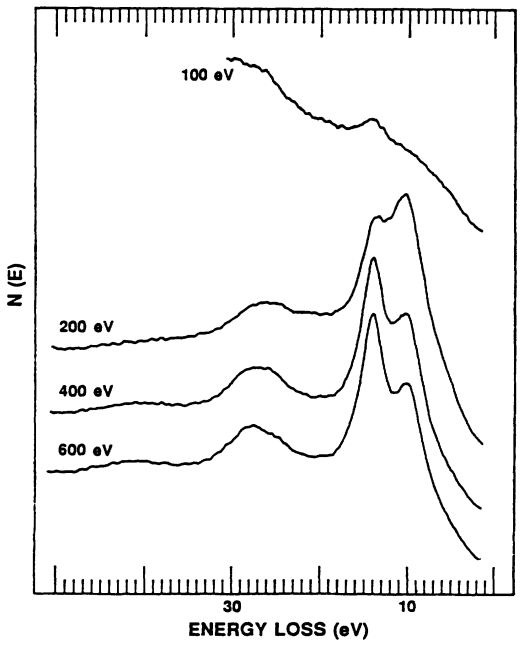

FIG. 2. EELS spectra obtained from polycrystalline Sn after exposure to 100 L of O_2 using primary-beam energies of 100, 200, 400, and 600 eV.

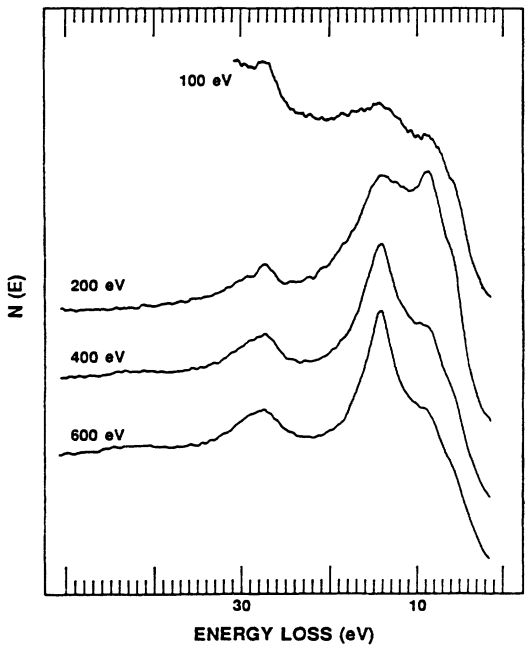

FIG. 4. EELS spectra obtained from polycrystalline Sn after exposure to 1500 L of O_2.

clean Sn metal are also shown in these figures.

The EELS spectra obtained after the 100-L O_2 exposure and shown in Fig 2 are quite similar to those obtained from the clean Sn. This is expected based on the discussion above since the metallic-plasmon-loss features are so large compared to the oxidic-loss features and the 100-L exposure results in the adsorption of a small amount of O. However, comparison of these spectra with the corresponding spectra shown in Fig. 3 of the previous part of this study[16] or in Figs. 8–11 shows that the metallic surface-plasmon peak at 10 eV is reduced in size with respect to the metallic bulk-plasmon peak after the 100-L exposure in the spectra obtained using primary-beam energies of 200, 400, and 600 eV. This is expected since chemisorption of submonolayer quantities alters the density of conduction electrons in the near-surface region.

The 100-eV EELS spectrum is more complex and needs to be considered along with the 100-eV EELS spectra that were obtained from clean Sn and 50-L-dosed Sn and are shown in Fig. 8. The 100-eV EELS spectrum obtained from clean Sn contains several features, all of which are quite small in absolute magnitude. The predominant feature is the bulk plasmon at 14 eV, and only a very small surface plasmon is present as a shoulder at 10 eV. This is unexpected since a 100-eV primary-beam energy should yield a highly surface-sensitive spectrum with a large surface plasmon as found by Bayat-Mokhtari, Barhovv, and Gallon.[20] However, their tin layer was evaporated onto a hot (100°C) substrate and not ion sputtered like the sample used in this study. The ion bombardment apparently has disrupted the structural arrangement of the Sn atoms in the near-surface region sufficiently to disrupt the conduction-band electrons so that they do not yield a significant surface-plasmon loss feature. If this assertion is correct, then it is an important finding because few techniques are capable of detecting surface damage in the outermost few atomic layers. Further research on this topic is in progress. The broad distribution of features ranging from 23 to 30 eV probably is not due to multiple plasmon losses in this case but

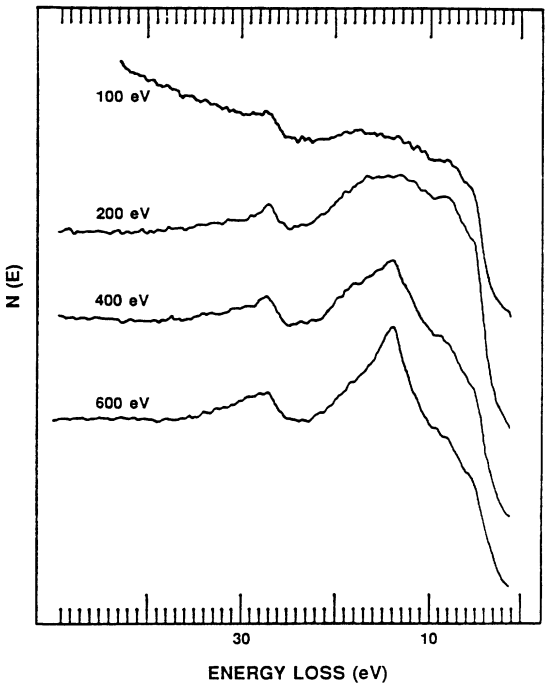

FIG. 6. EELS spectra obtained from polycrystalline Sn after an O_2 exposure of 160 Torr for 5 min.

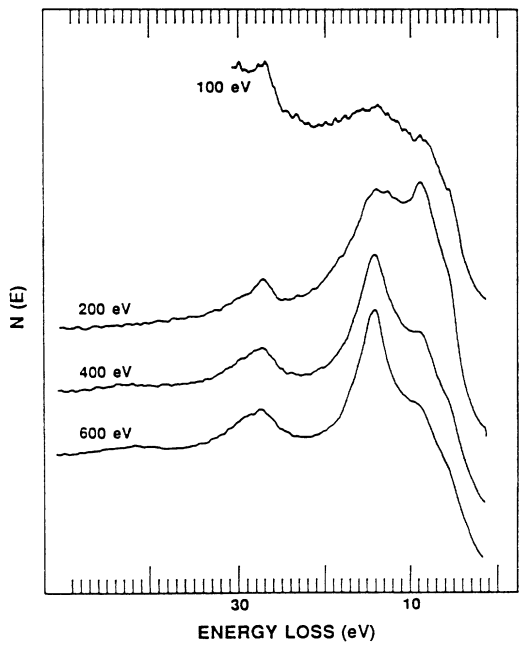

FIG. 5. EELS spectra obtained from polycrystalline Sn after exposure to 3500 L of O_2.

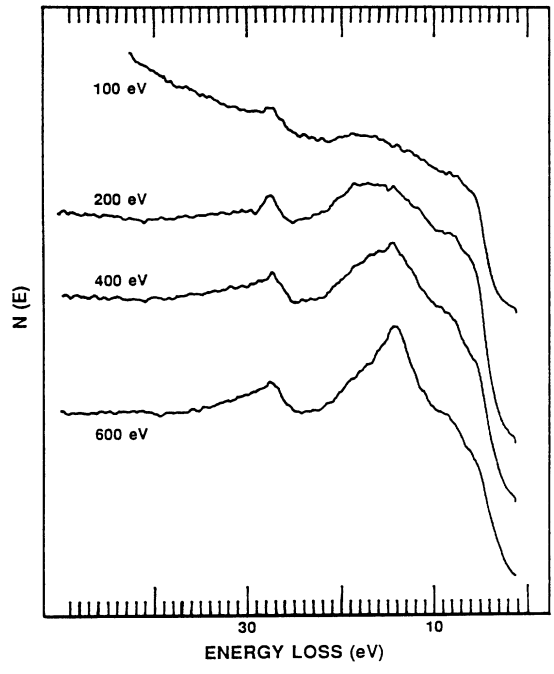

FIG. 7. EELS spectra obtained from polycrystalline Sn after an air exposure for 5 min.

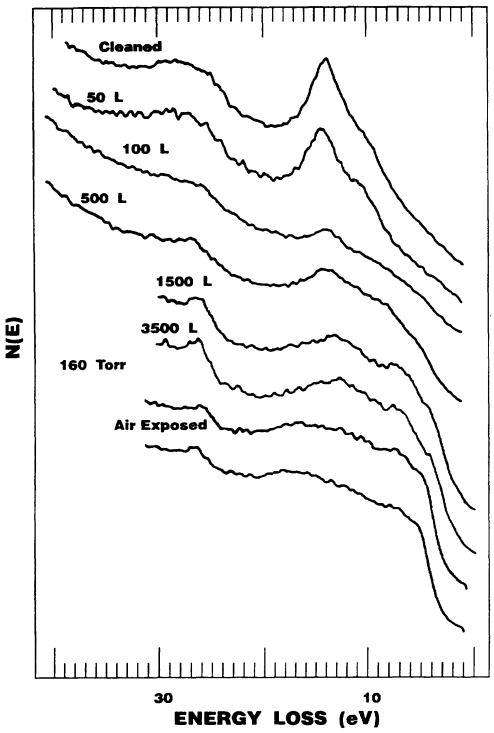

FIG. 8. EELS spectra obtained from cleaned and oxygen-exposed polycrystalline Sn using a primary-beam energy of 100 eV.

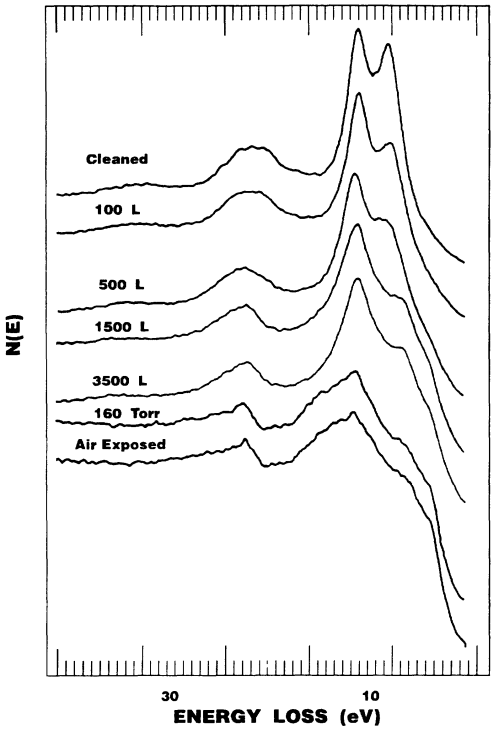

FIG. 10. EELS spectra obtained from cleaned and oxygen-exposed polycrystalline Sn using a primary-beam energy of 400 eV.

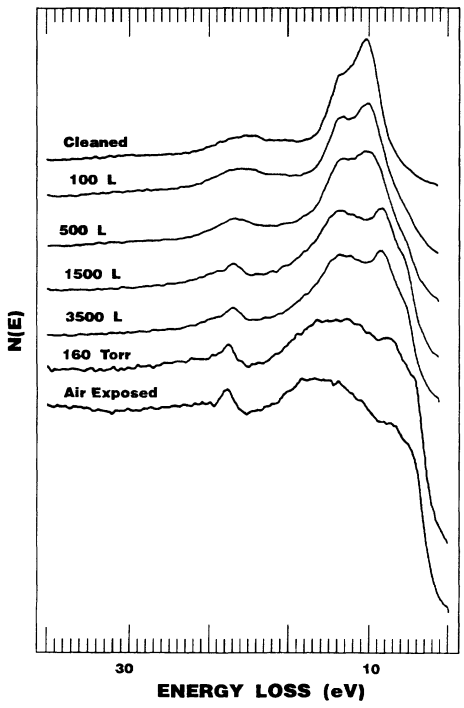

FIG. 9. EELS spectra obtained from cleaned and oxygen-exposed polycrystalline Sn using a primary-beam energy of 200 eV.

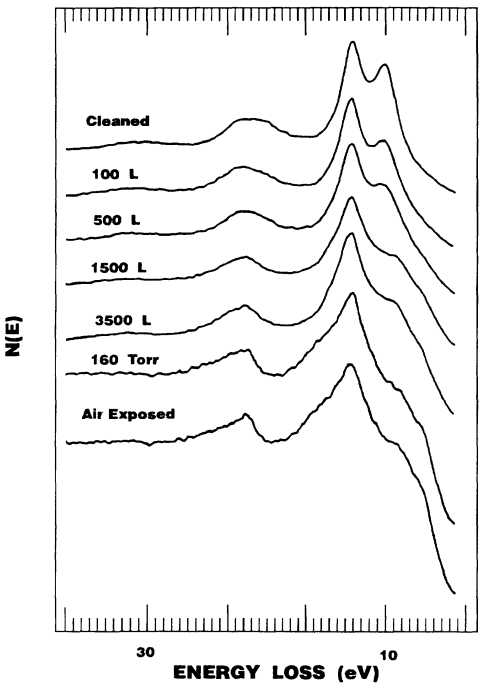

FIG. 11. EELS spectra obtained from cleaned and oxygen-exposed polycrystalline Sn using a primary-beam energy of 600 eV.

rather to interband transitions from the Sn 4*d* states to low-lying unfilled conduction-band levels. This seems quite reasonable since the Sn 4*d* $\frac{5}{2}$ and $\frac{3}{2}$ levels lie about 23 and 24 eV below the Fermi level. Thus, the threshold for this loss mechanism would lie at 23 eV. The energy range would be several eV since many of the Sn 4*d* electrons would be excited to higher-lying levels in the unfilled conduction band. The intensity of this feature is small so it is only prominent when other peak intensities are small, as in this case of using low-primary-beam energies to examine rough surfaces. Similar core-to-conduction-band transitions for tin oxides have been discussed by Cox and Hoflund.[12]

Significant changes occur in the 100-eV loss spectrum after just a 50-L exposure, as shown in Fig. 8. The intensities of all features decrease particularly in the 23–30-eV region, and shoulders form on both of the plasmon peaks at 9 and 13 eV due to formation of SnO. The changes in the 100-L loss spectrum become more extensive as the metallic features decrease in size and the SnO features become more prominent. A narrowing of the broad peak due to Sn 4*d*-to-conduction-band transitions can also be observed as a well-defined 27-eV peak forms due to the presence of SnO.

Further changes occur with increasing exposure, and the extent of the changes are greater in the near-surface region probed by the lower primary-beam energies. For the larger exposures the changes in the EELS spectra taken using higher primary-beam energies become more discernible. This can be observed in the EELS data taken after the 500-L exposure and shown in Fig. 3. In the 100-eV EELS spectrum, the 27-eV peak has become very well defined, and other SnO features at 9 and 13 eV have become more prominent. Also, a peak at 5.5 eV has become fairly distinct. This feature appears in all of the SnO-like spectra of the previous study,[12] and based on the energy-level diagram given in Fig. 1 of that study, this feature is probably due to an interband excitation from O 2*p* lone-pair electrons across the oxide band gap to unfilled conduction-band levels. The features due to metallic Sn are suppressed further after the 500-L exposure, particularly in the 100-eV EELS spectrum. Very interesting changes also occur in the EELS spectra obtained using higher primary-beam energies of 200, 400, and 600 eV. The surface-plasmon intensity is decreased, which causes a change in shape in the multiple-plasmon-loss region from 24 eV (surface-bulk loss) to 28 eV (bulk-bulk loss). As expected, the intensity near 24 eV decreases with respect to the intensity near 28 eV. This is particularly noticeable in the 600-eV EELS spectra presented in Fig. 11. The 27-eV loss feature also becomes more prominent after the 500-L exposure. This is more noticeable in the 200-eV spectra shown in Fig. 9. As the surface-plasmon-peak intensity decreases, the peak in this region broadens due to formation of SnO yielding signals at 9 and 13 eV so the valley between the metallic surface and bulk plasmons tends to become less pronounced.

A very important observation can be made by considering the 200-eV loss spectrum taken after the 500-L exposure. A fairly prominent shoulder is present at about 18 eV. As described above, Cox and Hoflund[12] attributed EELS structure at this loss energy to an O-deficient, SnO_2-like phase, which probably exists at boundaries between SnO_2 and SnO phases. The fact that this feature is observed after the 500-L exposure indicates that such a phase is forming and behaves as a precursor to SnO_2 formation. Furthermore, the fact that this feature appears in the 200-eV spectrum and not the 100-eV spectrum indicates that this phase lies beneath the surface but not so deeply that it contributes significantly to the 400- or 600-eV EELS spectra.

EELS spectra obtained after the 1500-L exposure are shown in Fig. 4. The trends described in the EELS spectra for the 500-L exposure have all continued and progressed much further during the 1500-L exposure. In the 100-eV spectrum the 27-eV SnO loss feature is distinct and well defined, and features due to the Sn 4*d*-to-conduction-band transitions are no longer apparent. The metallic bulk-plasmon feature at 14 eV still appears but is poorly defined due to the presence of SnO features. The metallic-surface-plasmon feature at 10 eV is not present, but a well-defined SnO surface plasmon at 9 eV has formed. The SnO interband transition at 5.5 eV is now quite distinct and is present in all four spectra in Fig. 4.

A very large change has also occurred in the 200-eV loss spectrum by increasing the exposure from 500 to 1500 L. The 9-eV SnO surface-plasmon-loss feature has become predominant whereas it is barely apparent in the 200-eV loss spectrum obtained from the 500-L-dosed surface. Also, the SnO 27-eV loss feature has sharpened considerably. The metallic Sn bulk plasmon peak at 14 eV is apparent, but it is broadened to higher binding energy losses due to increased intensity of the 18-eV feature. Some structure is now present at 19.5 eV indicating the formation of a subsurface SnO_2 phase. Both the transitional phase responsible for the 18-eV intensity and the SnO_2 phase are less apparent in the 400-eV spectrum and contribute only slightly to the 600-eV spectrum. The SnO feature at 9 eV contributes less to the 400- and 600-eV spectra, but this feature is still distinct and prominent in both spectra as is the 5.5-eV feature. Similarly, the 27-eV peak can be discerned in the 400-, and 600-eV loss spectra but diminishes in strength as the primary-beam energy increases.

EELS spectra taken after an O_2 exposure of 3500 L are shown in Fig. 5. This exposure is the saturation exposure with regard to EELS data since larger exposures yield EELS data essentially identical to those obtained after a 3500-L exposure. Oxygen most certainly continues to absorb after 3500 L but most likely at a very low rate resulting in negligible change in the EELS spectra. In fact, the EELS spectra taken after the 3500-L exposure are quite similar to those taken after the 1500-L exposure so only the differences between the two sets of spectra are described. The 100-, and 200-eV spectra for the two exposures are essentially identical, but the SnO 9-eV feature is somewhat more pronounced in the 400-eV spectrum after the 3500-L exposure. This feature becomes even more pronounced in the 600-eV spectrum, and the 27-eV peak also sharpens. These fairly subtle differences indicate that a fairly small amount of O has adsorbed in increasing the exposure from 1500 to 3500 L and that this O

penetrates deeply beneath the surface. These data also indicate that an oxide layer forms that protects the subsurface metal layers from further oxidation because the rate of O permeation through the oxide layer is very slow.

The EELS data and related discussion above regarding polycrystalline Sn exposed to O_2 at low pressure ($\sim 10^{-6}$ Torr) resolve a dilemma posed by Powell.[2] From the EELS data obtained using a 400-eV primary beam, he concluded that SnO is the only oxide formed on polycrystalline surfaces after exposure to low-pressure O_2. However, his UPS data show that both SnO and SnO_2 are present on the same surface. The presence of both SnO and SnO_2 according to EELS has been verified in this present study by varying primary-beam energy and observing changes in the spectra as the depth sensitivity changes thereby providing consistency between the EELS and UPS results. The fact that SnO_2 is more easily identifiable in UPS data than EELS data is probably due to differences in cross sections or relative sensitivity factors relating to the fundamental processes involved in the two techniques rather than to differences in inelastic mean free paths, as originally suggested by Powell.

EELS spectra taken from the Sn sample after high-pressure O_2 exposures are shown in Figs. 6 and 7. The data shown in Fig. 6 were taken after a 5-min exposure to high-purity O_2 at a pressure of 160 Torr in a sample preparation chamber attached to the UHV characterization chamber so that air exposure was avoided in this case. The data shown in Fig. 7 were taken after a 1-atm exposure to moist air by admitting the air into the preparation chamber. Care was taken so that the actual O_2 exposures in both cases were the same. In essence, this allows the rates of oxidation under dry and moist conditions to be compared.

Clearly, the EELS spectra obtained after high-pressure exposures are very different from those obtained after low-pressure exposures. The 100-eV loss spectrum in Fig. 6 contains no distinct 14-eV metallic bulk-plasmon loss feature indicating the absence of metallic Sn in the near-surface region. Several well-defined SnO features do appear at 5, 9, 13, and 27 eV. However, the 9-eV feature apparently has shifted to 8-eV, which is consistent with EELS spectra obtained from more fully oxidized samples. Most importantly, the transitional phase between SnO and SnO_2 exhibits a fairly distinct peak at 18 eV with a small shoulder at 20 eV. This suggests that some SnO_2 lies quite near to the surface. With increasing primary-beam energy, the 18-eV feature and 20-eV shoulder increase in intensity, indicating that the subsurface regions are more fully oxidized than the near-surface region. These features are of less importance in the 600-eV loss spectrum, but a small 18-eV loss feature is still present. The SnO features persist throughout the whole energy range but also become less important in the 600-eV loss spectrum. A prominent metallic bulk-plasmon loss peak appears in the 400-eV spectrum and has increased intensity in the 600-eV loss spectrum. Although the peaks are quite small, it appears that two separate and distinct peaks are present at 8 and 9 eV. This may imply that the 9-eV peak did not shift to 8 eV but that the peaks originate from different phases, i.e., the 9-eV peak from SnO and the 8-eV peak from either the transitional phase or SnO_2.

The EELS spectra obtained after the air exposure and shown in Fig. 7 are quite similar to those shown in Fig. 6 with one very important difference. The intensities of the 18- and 20-eV features in each corresponding spectrum are greater. The 200-eV loss spectrum actually exhibits a distinct 20-eV SnO_2 feature rather than just a shoulder. These data indicate that the extent of oxidation is greater for the air-exposed surface. Furthermore, this implies that moisture accelerates the rate of oxidation in some manner.

In an early study of the oxidation of Sn, Powell and Spicer[13] suggested that after exposure to O_2 the outermost surface layer consists of metallic Sn. In the following paper,[2] Powell reasserts his belief that Sn metal exists at the surface after O_2 exposure, states that this assertion cannot be verified based on his UPS, AES, and EELS data, and also states that the coexistence and distribution of Sn metal and oxides in the near-surface region remains an open question. Based on the studies by Cox and Hoflund,[12] Asbury and Hoflund,[1] Hoflund and Corallo,[16] and the data presented in this study, fairly detailed answers can now be given to the important questions raised by Powell. In the study by Asbury and Hoflund,[1] ion scattering spectroscopy (ISS), AES, and ESCA were used to demonstrate that O readily penetrates beneath a metallic surface during oxidation at either low or high pressure. The fact that a significant ISS O peak was not formed during any exposure was interpreted as due to the absence of a significant amount of O in the outermost atomic layer. This interpretation requires reassessment based on a recent study of O chemisorption on polycrystalline Ag by Davidson, Hoflund, and Outlaw.[22] Using the same ISS apparatus as that used to examine the O/Sn system, they performed an ISS cross-section calibration study and found that the O/Ag cross-section ratio is about 0.05. Since the atomic mass of Ag is similar to that of Sn, the cross-section ratio should be of similar magnitude for the O/Sn system. Based on the relative peak heights of the O and Sn peaks in the ISS spectra presented by Asbury and Hoflund,[1] the Sn surface apparently consists of about 50% O for all of the exposures used. Therefore, it appears that the outermost layer of surface atoms at a Sn surface rapidly saturates with O and then more adsorbing O penetrates beneath the surface. This interpretation is consistent with the surface-sensitive, 100-eV loss spectra presented in this study, which show that both SnO and Sn metal are present in the outermost four or five atomic layers. Furthermore, the SnO probably exists as islands at very low exposures since collective-mode oscillations appear in the EELS spectra for both SnO and Sn metal. This conclusion is in agreement with similar results and statements made by Bevolo, Verhoeven, and Noack.[5] The EELS data show that O, which penetrates beneath the surface, continues to form subsurface SnO until the O concentration is large enough for formation of the transitional phase, which acts as a precursor for SnO_2 formation at even larger subsurface O concentrations.

The same mechanisms appear to hold for oxidation of a Sn surface at higher pressures and greater exposures, but in this case the outermost atomic layer is more fully oxidized so that metallic Sn is not present. Also, the extent of oxidation is much greater, resulting in the formation of more SnO_2 in the subsurface region. Powell did not examine such surfaces in his studies. At this point is it not known if any oxidative conditions could be found which would lead to complete oxidation of the near-surface region of Sn to SnO_2.

It has been demonstrated in a well-controlled experiment that increasing the primary-electron-beam energy increases the sampling depth probed in EELS.[16] Thus, Figs. 2–7 contain chemical-state information as a function of depth, i.e., they can be considered to be chemical-state depth profiles. By quantifying the relative amounts of Sn metal, SnO, and SnO_2 present based on the intensities of the features described above and calculating the sampling depth as a function of primary-beam energy, it is possible to construct a semiquantitative plot of the average Sn oxidation state as a function of depth for the various exposures. This has been done, and the results are shown in Fig. 12. The sampling depth was determined based on the first-order term in the Poisson distribution

$$P(1)=\left[\frac{d}{\lambda}\right]e^{-(d/\lambda)}, \tag{1}$$

which is related to the probability that one inelastic collision will occur in depth d where λ is the inelastic mean free path. Taking into account the experimental geometry and Eq. (1), the EELS sampling depth is given by

$$d=\frac{(4.5)\lambda\cos X\cos Y}{\cos X+\cos Y}, \tag{2}$$

where X is the incidence angle and Y is the collection angle. In this case d is defined as the depth from which 95% of the inelastically scattered electrons are collected. Values of λ used and calculated sampling depths are given in Table I. This simplistic approach has problems

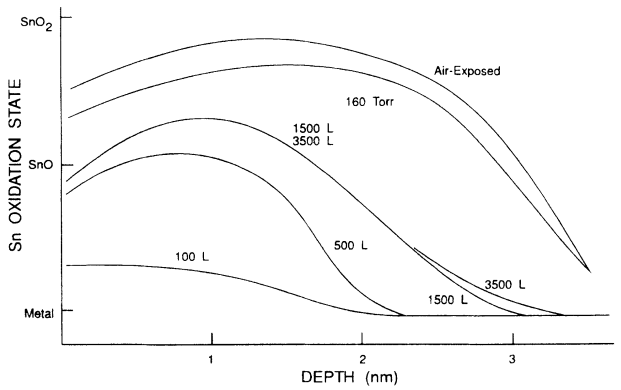

FIG. 12. Semiquantitative depth profile of the Sn chemical state of oxygen-exposed polycrystalline Sn as a function of exposure.

TABLE I. EELS sampling depths for clean and oxidic Sn.

	Clean Sn		Oxidic Sn	
E_p (eV)	λ (nm)	d (nm)	λ (nm)	d (nm)
100	0.7	1.0	1.0	1.4
200	1.0	1.3	1.4	1.9
400	1.4	1.9	1.9	2.6
600	1.6	2.3	2.3	3.2

in that it assumes a simple cosine dependence on incidence and collection angles and strong variations in λ based on the spatial distributions of the chemical species in the surface region are neglected but, nevertheless, a semiquantitative plot is obtained that summarizes the EELS results of Figs. 2–7.

At low pressures and low exposures, O adsorbs on the surface and some of it penetrates beneath the surface forming SnO or a suboxide. The O remaining in the outermost atomic layer may be in a chemisorbed rather than oxidic form, as discussed in a study of O-exposed Pt_3Sn alloy surfaces by Asbury and Hoflund.[23] As the exposure is increased, more O accumulates in the near-surface region and also penetrates further beneath the surface. The average Sn oxidation state increases particularly beneath the surface where the transition lattice forms and then proceeds to formation of SnO_2 with increasing O exposure. The profiles obtained from the 1500- and 3500-L exposures are quite similar except at a depth of about 3.0 nm, where the 3500-L-exposed surface contains more SnO. Both of these exposures leads to the formation of SnO_2 at an average depth of about 1.0 nm beneath the surface. The near-surface region contains a metallic Sn phase but is mostly SnO.

The high-pressure exposures result in a 3.0-nm-thick layer of mostly SnO and SnO_2. The near-surface region contains no metallic Sn and consists of a mixture of SnO mostly with some transitional phase and a little SnO_2. A large amount of SnO_2 is present beneath the surface, and the transitional phase and SnO lie beneath the SnO_2 where the concentration of metallic Sn increases until bulk metal is reached. The presence of moisture appears to enhance the rate of oxidation.

Another way of varying the depth sensitivity of EELS is to vary the incident and collection angles as described by Hoflund and Corallo.[16] This has an advantage over varying depth sensitivity by changing primary-beam energy because the cross-sectional variation of EELS features with energy is not a consideration when a constant primary-beam energy can be used. ARELS data taken from the polycrystalline Sn surface after dosing with 3500 L at $\sim 10^{-6}$ Torr are shown in Fig. 13. The spectra were taken using a 200-eV primary-beam energy, an incident angle X of 45°, and the collection angle Y shown by each spectrum. All angles are given with respect to the sample normal which is defined as 0°. The top spectrum is the most sensitive, the middle spectrum is the same 200-eV spectrum shown in Fig. 5, and the lowest spectrum is the most bulk sensitive. Based on Eq. (2), the surface-sensitive spectrum probes about 8 Å, and

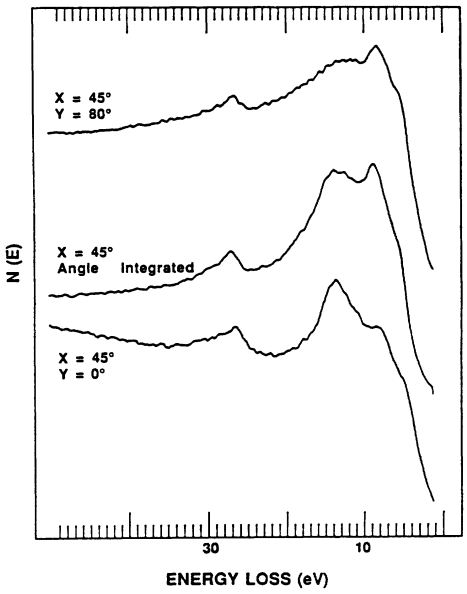

FIG. 13. ARELS spectra taken from a polycrystalline Sn surface after dosing with 3500 L of O_2 at 10^{-6} Torr. The spectra were taken using a 200-eV primary beam, an incidence angle X of 45°, and the collection angle Y shown by each spectrum. The upper spectrum is the most surface sensitive of the three, and the lowest is the most bulk sensitive.

the bulk-sensitive spectrum probes about 25 Å. According to Table I, the middle spectrum probes about 19 Å. Therefore, the surface-sensitive ARELS spectrum probes about one-half the depth of the 100-eV spectrum shown in Fig. 5. The most noticeable differences are that the 14-eV Sn metal bulk-plasmon peak is greatly reduced and the SnO features at 8.4, 13, and 27 eV are more prominent in the more highly surface-sensitive ARELS spectrum. These data indicate that the outermost two atomic layers of 3500-L O_2-exposed polycrystalline Sn consists primarily of SnO and very little, if any, metallic Sn. Compared to the surface-sensitive spectrum, the spectrum obtained by collecting all electrons in the 360° cone (middle, angle-integrated spectrum in Fig. 13 probing about 19 Å) exhibits an enhanced 14-eV metallic Sn bulk-plasmon feature, enhanced structure in the 18–20-eV region and the 30-eV region due to the presence of the transitional phase and SnO_2, and a broadened 27-eV feature. These facts indicate that Sn metal, SnO, SnO_2 and the transitional phase are all present in the outermost 19 Å of this surface. Since the cross sections of the metallic Sn features are much larger than those of the oxidic features, metallic Sn is present in this region in fairly small quantities. The more bulk-sensitive ARELS spectrum shown in Fig. 13, which probes a depth of about 25 Å, is quite similar to the 400-eV spectrum shown in Fig. 5, which probes a depth of 26 Å. As expected, the metallic Sn features are even more prominent in the more bulk-sensitive ARELS spectrum. These ARELS spectra allow for two important points to be made. Firstly, the top ARELS spectrum in Fig. 13 is the most highly surface-sensitive spectrum obtained in this study. It provides clear evidence that the very near-surface region of a Sn surface saturated with O at low pressure consists essentially of SnO with no Sn metal or SnO_2 present. Secondly, the ARELS results are in complete agreement with the results obtained by varying the primary-beam energy. This fact supports the assertions that meaningful depth-sensitive chemical-state information can be obtained from EELS using this general approach and that the interpretation of the EELS spectra is correct.

SUMMARY

EELS has proven to be a very powerful technique for obtaining depth-sensitive, chemical-state information during the oxidation of polycrystalline Sn metal at room temperature. Such information cannot be obtained using more conventional techniques such as AES and ESCA. Depth sensitivity has been provided in this study primarily by varying the primary-beam energy, but similar information has been obtained by performing ARELS. EELS is very sensitive to differences in chemical states because particle excitations depend upon both the filled and empty density of electronic states near the Fermi level, i.e., the valence region, which is strongly dependent upon the chemical environment, and the collective-mode oscillations, which also are sensitive to the bonding characteristics of the nearly free electrons. Thus, EELS exhibits distinct and discernible features for Sn metal, SnO, SnO_2, and a transition phase which is a precursor to SnO_2 formation. This important information allows for a determination of the chemical state of the Sn as a function of depth for various O_2 exposures. The EELS data and compositional depth profiles have been used to formulate a model for the oxidation of Sn. The development of this model was possible because extensive EELS data were taken over broad ranges of primary-beam energies and O_2 exposures. It is consistent with many previous suggestions regarding the oxidation of Sn, clarifies some earlier controversies and inconsistencies, and provides a general and powerful technique for studying the oxidation of metals.

ACKNOWLEDGMENT

Support for this research was provided by the National Science Foundation through Grant No. CTS-9122575.

[1]D. A. Asbury and G. B. Hoflund, J. Vac. Sci. Technol. A **5**, 1132 (1987).
[2]R. A. Powell, Appl. Surf. Sci. **2**, 397 (1979).
[3]C. M. Stander, Appl. Surf. Sci. **16**, 463 (1983).
[4]A. J. Bevolo, J. D. Verhoeven, and M. Noack, J. Vac. Sci. Technol. **20**, 943 (1982).
[5]A. J. Bevolo, J. D. Verhoeven, and M. Noack, Surf. Sci. **134**, 499 (1983).
[6]P. Sen, M. S. Hegde, and C. N. R. Rao, Appl. Surf. Sci. **10**, 63 (1982).
[7]M. E. Woods and B. J. Hopkins, J. Phys. C **18**, 3255 (1985).
[8]C. L. Lau and G. K. Wertheim, J. Vac. Sci. Technol. **15**, 622

(1978).
[9]A. M. C. Lin, N. R. Armstrong, and T. Kuwana, Anal. Chem. **49**, 1228 (1977).
[10]W. E. Morgan and J. R. Van Wazer, J. Phys. Chem. **77**, 964 (1973).
[11]E. Paparazzo, G. Fierro, G. M. Ingo, and N. Zacchetti, Surf. Interf. Anal. **12**, 438 (1988).
[12]D. F. Cox and G. B. Hoflund, Surf. Sci. **151**, 202 (1985).
[13]R. A. Powell and W. E. Spicer, Surf. Sci. **2**, 55 (1976).
[14]S. K. Sen, S. Sen, and C. L. Bauer, Thin Solid Films **82**, 157 (1981).
[15]C. D. Wagner and P. Biloen, Surf. Sci. **35**, 82 (1973).
[16]G. B. Hoflund and G. R. Corallo, Surf. Interf. Anal. **13**, 33 (1988).
[17]R. E. Gilbert, D. F. Cox, and G. B. Hoflund, Rev. Sci. Instrum. **53**, 1281 (1982).
[18]G. B. Hoflund, D. F. Cox, G. L. Woodson, and H. A. Laitinen, Thin Solid Films **78**, 357 (1981).
[19]M. J. Tarlov and J. F. Evans, Chem. Mater. **2**, 49 (1990).
[20]P. Bayat-Mokhtari, S. M. Barhovv, and T. E. Gallon, Surf. Sci. **83**, 131 (1979).
[21]G. Rasigni, J. P. Codaccioni, J. Michaud-Bonnet, F. Abba, and J. P. Petrakian, Compt. Rend. (Paris) B **262**, 772 (1966).
[22]M. R. Davidson, G. B. Hoflund, and R. A. Outlaw, J. Vac. Sci. Technol. A **9**, 1344 (1991).
[23]D. A. Asbury and G. B. Hoflund, Surf. Sci. **199**, 552 (1988).